LA-UR-10-00874

Approved for public release; distribution is unlimited.

Title: Production of ultracold neutrons from cryogenic 2H2, O2, and C2H4 converters

Author(s): F. Atchison, B. Blau, K. Bodek, B. van den Brandt, T. Brys, M. Daum, P. Flerlinger, A. Frei, P. Geltenbort, P. Hautle, R. Henneck, S. Heule, A. Holley, M. Kasprzak, K. Kirch, A. Knecht, J. A. Konter, M. Kuzniak, C.-Y. Liu, C. L. Morris, A. Pichlmaier, C. Plonka, Y. Pokotilovski, A. Saunders, Y. Shin, D. Tortorella, M. Wohlmuther, A. R. Young, J. Zejma, G. Zsigmond

Intended for: Publication – Physical Review Letters

Los Alamos
NATIONAL LABORATORY
EST. 1943

Los Alamos National Laboratory, an affirmative action/equal opportunity employer, is operated by the Los Alamos National Security, LLC for the National Nuclear Security Administration of the U.S. Department of Energy under contract DE-AC52-06NA25396. By acceptance of this article, the publisher recognizes that the U.S. Government retains a nonexclusive, royalty-free license to publish or reproduce the published form of this contribution, or to allow others to do so, for U.S. Government purposes. Los Alamos National Laboratory requests that the publisher identify this article as work performed under the auspices of the U.S. Department of Energy. Los Alamos National Laboratory strongly supports academic freedom and a researcher's right to publish; as an institution, however, the Laboratory does not endorse the viewpoint of a publication or guarantee its technical correctness.

Form 836 (7/06)

Production of ultracold neutrons from cryogenic $^2H_2$, O_2, and $C\,^2H_4$ converters

F. Atchison,[1] B. Blau,[1] K. Bodek,[2] B. van den Brandt,[1] T. Bryś,[1,*] M. Daum,[1] P. Fierlinger,[1,†] A. Frei,[3] P. Geltenbort,[4] P. Hautle,[1] R. Henneck,[1] S. Heule,[1,‡] A. Holley,[5] M. Kasprzak,[1,§] K. Kirch,[1,¶] A. Knecht,[1,‡] J. A. Konter,[1] M. Kuźniak,[2,**] C.-Y. Liu,[6] C. L. Morris,[7] A. Pichlmaier,[1] C. Plonka,[4] Y. Pokotilovski,[8] A. Saunders,[7] Y. Shin,[6] D. Tortorella,[3] M. Wohlmuther,[1] A. R. Young,[5] J. Zejma,[2] and G. Zsigmond[1]

[1] *Paul Scherrer Institut (PSI), CH-5232 Villigen PSI, Switzerland*
[2] *Institute of Physics, Jagiellonian University, Cracow, Poland*
[3] *Technische Universität München, München, Germany*
[4] *Institut Laue-Langevin (ILL), Grenoble, France*
[5] *North Carolina State University, Raleigh, U.S.A.*
[6] *Indiana University, Bloomington, U.S.A.*
[7] *Los Alamos National Laboratory, Los Alamos, U.S.A.*
[8] *Joint Institute for Nuclear Research, Dubna, Russia*

(Dated: January 26, 2010)

Ultracold neutrons (UCN) have been produced using the cold neutron (CN) beam FUNSPIN at SINQ on cryogenic oxygen (O_2), tetradeuteromethane ($C\,^2H_4$), and deuterium ($^2H_2$) targets. The target cell (40 mm long, fiducial volume about 45 cm^3) was operated between room temperature and 8 K and UCN were produced from gaseous, liquid and solid targets. UCN rates have been measured as a convolution of UCN production and transport out of the target and to the detector. At least within the accessible temperature range of this experiment, deuterium outperforms the other materials.

PACS numbers: 28.20.-v Neutron physics, 28.20.Cz Neutron scattering, 61.12.Ex Neutron scattering

Efforts are underway worldwide to improve on the intensity and density of ultracold neutrons available to fundamental physics experiments [1]. The main two avenues use cold neutrons as an input onto a cryogenic converter, either superfluid helium [2] or solid ortho-deuterium [3]. Some ground breaking work, demonstrating the potential of solid deuterium has been reported in [4–7]. In connection with the construction of a powerful deuterium based UCN source at PSI, an extensive R&D program was pursued for the investigation of the relevant UCN source physics [8–14]. While different converter materials have been tested in the early days of UCN physics (see [15] for some history and references to the original work), the use of solid oxygen and solid tetradeuteromethane as potentially powerful UCN converters has been proposed only recently [16, 17].

A UCN converter should provide a large cross section for neutron "down-scattering" to lower energies, while at the same time "up-scattering" and absorption should be small or suppressed. While the down-scattering is governed by the available density of states, the up-scattering is affected by the actual population of excited states in a converter. This population can be influenced by temperature and one is lead to cryogenic materials for which, by detailed balance, a Boltzmann factor suppresses the up-scattering. It is usually helpful to characterize the properties of the converter by the UCN production rate R (dependant of the incoming neutron energy spectrum) and the UCN lifetime τ inside the converter material, such that the product with an incident cold neutron flux ϕ results in the equilibrium UCN density $\rho_{\rm UCN}$ inside the converter: $\rho_{\rm UCN} = R\phi\tau$. For deuterium $R \sim 10^{-8}\,{\rm cm}^{-1}$ has been calculated [3] and measured [10], while τ is limited to about 150 ms due to the unavoidable absorption of neutrons on deuterons. Practically, $\tau \sim 40$ ms [6] has been achieved experimentally so far. For superfluid helium, the production rate has also been calculated [2] and measured [18] and, for a typical cold neutron beam spectrum, is about 1 order of magnitude lower than for deuterium, but $\tau \sim 900$ s (corresponding to the free neutron lifetime) can in principle be obtained in pure superfluid ^{4}He.

For good UCN production performance, low loss materials (large τ) and systems with suitable down-scattering properties (large R) are required. The two novel cryogenic converter materials investigated in this work could fulfill these criteria. The absorption cross sections of the constituent nuclei are relatively small ($\sigma^{\rm O}_{\rm abs} \sim 0.2$ mbarn and $\sigma^{\rm C}_{\rm abs} \sim 3.5$ mbarn leading to unavoidable loss rates due to absorption of about 1/(400 ms) for O_2 and 1/(40 ms) for $C\,^2H_4$) while the down-scattering could potentially make use of many more low lying molecular states (for the case of $C\,^2H_4$) or the excitation of spin waves (for the case of O_2 in the antiferromagnetic α-phase). Contrary to the situation with superfluid helium and deuterium, where theoretical estimates were available at the time of the experiments, no conclusive predictions for the UCN production rates of O_2 and $C\,^2H_4$ exist to date.

The aim of this work was to test the UCN production performance of O_2 and $C\,^2H_4$ in comparison with $^2H_2$. The experiment was performed on the CN beam line for fundamental physics (FUNSPIN) [19] at the Swiss spallation neutron source SINQ. A schematic diagram of

the experimental setup is displayed in Fig. 1. The cryogenic and UCN parts were similar to the ones employed in [10], using the same gas system, cryogenic target (see also [20]), UCN detector and UCN guide system with only minor modifications. The relevant changes in the setup as compared to [10] were the use of a different first UCN mirror (an Al foil coated with diamond like carbon)) and a time–of–flight (TOF) system for CN behind the first UCN mirror. Typical resolutions of the TOF system were 1-5%. After passing a 38 mm aperture and a 125 μm Zr vacuum window, CN from the FUNSPIN beam entered the 40 mm long target. Downstream of the target, a UCN guide system (Ni coated stainless steel and Be coated glass) was mounted in which after roughly 0.6 m a first mirror separated UCN (and some very cold neutrons, see [10]) from the CN beam by reflecting them upwards. The UCN were again reflected by 90° by a second mirror at about 1 m height into a horizontal guide section perpendicular to the axis of the incident beam; this helped to further filter the UCN spectrum and reduced beam induced background in the detector system. UCN passed the 1.4 m long horizontal section and fell by about 1 m into a well shielded ^{3}He gas detector. In order to reach the TOF system, CN passed through the UCN mirror (100 μm Al with diamond like carbon coating), a 10 mm hole in the attached ^{6}LiF beam dump and a 100 μm Al vacuum exit window. The TOF system had a total flight path of 2830 mm and consisted of a one-disc-one-slit chopper (operated in air at 25 Hz and about 1/300 open to close ratio), a flight tube flushed with He to reduce neutron losses (2.5 m length, 16 μm Al entrance and exit windows), and a 'thin' CN detector (the same as used in [19]). 'Thin' refers to a small amount of ^{3}He in the counting gas which should result in a $1/v$ dependence of the detector efficiency on CN velocity v. The TOF system was used to monitor the CN beam intensity and spectrum. It also allowed measurement of the energy dependent CN attenuation for various target conditions from which one can calculate total scattering cross sections. These CN data have already been published in [14].

The produced UCN (in flow–through mode: both UCN shutters open) and transmitted CN have been detected for gaseous, liquid, and solid phases of $^2H_2$, O_2, and $C\,^2H_4$ at various temperatures. The information about temperatures of phase transitions have been collected in Table I. The data analysis follows the method used in [10] (for the measurements in the flow–through mode) with some modification due to e.g. a different normalization. Most notably, to determine the UCN production rates, I_m, in the sample, the number of detected UCN, N_{UCN}, is normalized to the transmitted CN counts, N_{CN}, measured at the same time:

$$I_m = (N_{UCN} - N_b)/N_{CN} \qquad (1)$$

where N_b is the background UCN rate measured with empty target. The rates I_m are shown in Fig. 2 for $^2H_2$, $C\,^2H_4$, and O_2 as a function of temperature. The rates I_m are the convolution of: (i) the downscattering cross section in the material σ^{CN-UCN}, (ii) the extraction efficiency ε_e, (iii) the transport efficiency ε_t which can be determined from the simulation. Since here the intention is to compare the UCN production in different materials, there is no need to determine the UCN production cross sections as was done for $^2H_2$ in [10]. However, we have to take into account various transport efficiencies of the UCN spectrometer due to different optical potentials of the investigated materials. The efficiencies ε_t are obtained by simulations carried out using the GEANT4 UCN-Monte Carlo code [21], which tracks UCN through a detailed model of the UCN spectrometer system. The extraction efficiencies ε_e may also differ due to various UCN lifetimes in the investigated materials. The target dimensions relevant for UCN extraction is less then 40 mm. Only if the UCN lifetime is shorter than the time needed to travel this typical distance, e.g. 40 mm / 5 m/s $\sim$ 8 ms, UCN loss in the target will considerably influence ε_e. Here we assume that ε_e is not affected. This assumption is based on the fact that the UCN extraction in case of solid $^2H_2$ is not influenced by specific details of the crystal but by the UCN lifetime in solid $^2H_2$ which is dominated by thermal upscattering. It is highly prob-

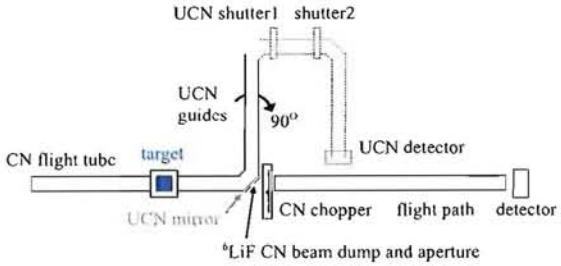

FIG. 1: The schematical setup (not to scale): The CN beam comes along a flight tube and hits the cryogenic target. Behind the target, UCN are reflected upwards by a mirror which is transparent for CN. The major part of the CN beam is dumped behind the mirror while the central fraction passes to the time–of–flight detection system. The UCN are simultaneously guided away from the CN beam axis to a well shielded UCN detector (compare [10]).

TABLE I: Properties of $^2H_2$, O_2 and $C\,^2H_4$: temperatures [K] of phase transitions and neutron optical potentials V_F (Fermi potentials) of the solids.

	$^2H_2$	$C\,^2H_4$	O_2
Boiling point	23.5	112	90.2
Melting point	18.7	89.9	54.8
		27.1<I<89.9	43.8<γ<54.4
Solid Phases		22.1<II<27.1	23.9<β<43.8
		III < 22.1	α < 23.9
V_F [neV]	$\sim$ 100	$\sim$ 177	$\sim$ 87

able that this will be also the case for solid $C\,^2H_4$ and O_2. The capture contribution for O_2 is negligible, and for $C\,^2H_4$, is slightly higher than for $^2H_2$. The upscattering coming from rotational excitations will also influence the UCN lifetime (see [22]), especially in $C\,^2H_4$, since the energy levels are much lower than for $^2H_2$ (see [17]). However, at low temperatures around 8 K, this contribution might be comparable with the thermal upscattering due to phonons. Certainly measurements of UCN lifetimes in solid $C\,^2H_4$ and O_2 are indicated. Here we implicitly assume that they are longer than $\sim$ 8 ms at 8K. Experimental confirmation is due to the temperature dependence of I_m (see Fig. 2) which is flat (O_2) or flattening at low temperature ($C\,^2H_4$).

Therefore, we correct the measured UCN production rates I_m only for the transport efficiencies. We introduce the function $T(v)$ to include the dependence of the average UCN production cross section $\bar{\sigma}(v_f)$ on the final neutron velocity v_f, $\bar{\sigma}(v_f) = \bar{\sigma}^{CN\to UCN} f(v_f)$ where, $f(v) \sim v^2$, so that:

$$T(v) = f(v)\varepsilon_t(v) \tag{2}$$

with the normalization condition

$$\int_{v_1}^{v_2} f(v)dv = 1 \tag{3}$$

where v_1 and v_2 are the velocities *in* the target material that lead to UCN storable in the bottle (< 250 neV). The distributions $T(v)$ for solid $^2H_2$, $C\,^2H_4$ and O_2 are shown in Fig. 3. To calculate the correction factors, functions $T(v)$ are integrated over the neutron velocity range that contributes to the UCN stored in the bottle. For solid $^2H_2$ ($V_F \sim 100$ neV [12]) the neutron velocity lies in the velocity range 0 to 6.8 m/s (corresponding to the energy range 0–250 neV) and

$$T_{^2H_2} = \int_0^{6.8\ \mathrm{m/s}} T(v)_{^2H_2} dv = 0.039 \tag{4}$$

In case of solid $C\,^2H_4$ at 8K with the optical potential V_F of 177 neV the corresponding neutron velocity range is 0 to 5.8 m/s (energy range 0–173 neV):

$$T_{C\,^2H_4} = \int_0^{5.8\ \mathrm{m/s}} T(v)_{C\,^2H_4} dv = 0.031 \tag{5}$$

Solid O_2 at 8K has $V_F = 87$ neV and thus the velocity range is 1.6 to 7.1 m/s (energy range 13–263 neV):

$$T_{O_2} = \int_{1.6\ \mathrm{m/s}}^{7.1\ \mathrm{m/s}} T(v)_{O_2} dv = 0.041 \tag{6}$$

The corrected UCN rates I_c (corresponding to relative production cross sections) are calculated using:

$$I_c = I_m/T. \tag{7}$$

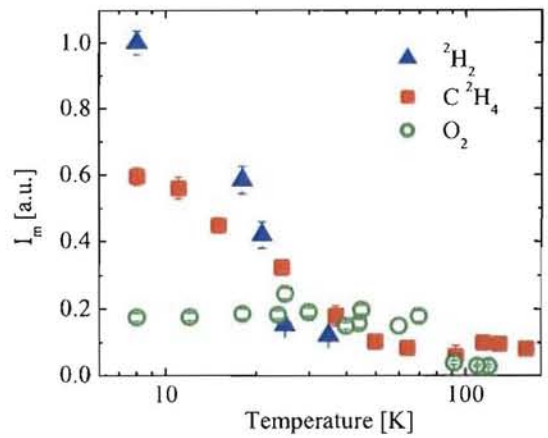

FIG. 2: The measured UCN production rates I_m for $^2H_2$, O_2 and $C\,^2H_4$ as a function of temperature of the cell. These rates are the detected UCN background corrected and normalized to the simultaneously detected, transmitted through the sample CN.

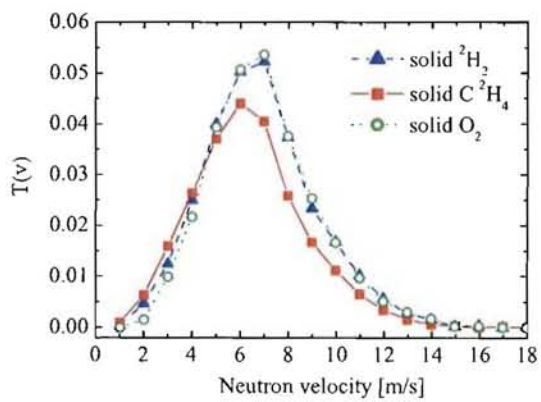

FIG. 3: The simulated transport efficiencies for solid $^2H_2$, O_2 and $C\,^2H_4$ inside the material. The simulation takes into account the Fermi potential of the materials.

TABLE II: UCN production rates I_c for solid $^2H_2$, O_2 and $C\,^2H_4$ at 8K, corrected for the transport efficiency.

Material	I_c
$^2H_2$	1.0 ± 0.04
$C\,^2H_4$	0.75 ± 0.03
O_2	0.17 ± 0.01

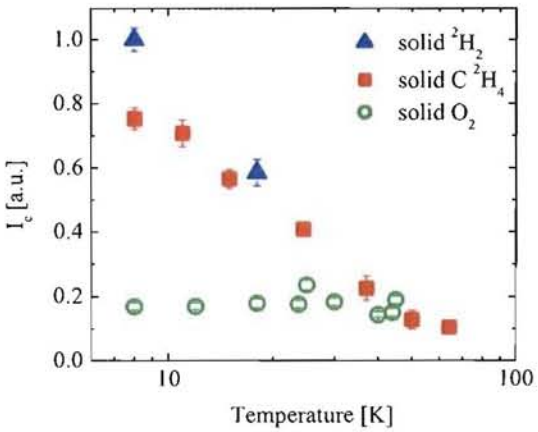

FIG. 4: The UCN production rates I_c for solid $^2H_2$, solid O_2 and solid C^2H_4. These rates are corrected for the transport efficiency (see Fig. 3) measured UCN rates I_m. The assumption made here is that the UCN extraction efficiencies are the same for all three materials.

and are shown in Figure 4 and for 8 K solids collected in Table II.

The results obtained show that the UCN production rate at 8K is the highest for solid $^2H_2$. The UCN production rate for solid C^2H_4 is 25 % lower and for solid O_2 at 8.0 K the rate is six times smaller. The low UCN production rate for solid O_2 might be explained by the lack of magnetic structure (spin waves) in the crystals grown. In this case, the only possible channel for UCN production would be via phonon excitations. Comparing the calculated UCN densities produced in solid $^2H_2$ and O_2 (see Fig. 7 in [16]), one can notice that the UCN density in solid O_2 without magnon excitations is about 6-7 times lower than for solid $^2H_2$. Important new insight from neutron scattering on solid O_2 [23] confirms that magnons do not contribute significantly under our conditions. Additionally, other issues appear in real UCN sources. Molecular carbon-containing moderators encounter significant difficulties in use at high-power steady state or pulsed neutron sources by radiation damage leading to destruction and polymerization [24]. Solid $^2H_2$ is much less affected by radiation heating compared to the heavier elements and thus it is better suited for high power sources, such as at PSI. Sources capable of further cooling to temperatures considerably below 8K might still benefit from other materials in case other down scattering channels would open up.

The work was performed at the Swiss Spallation Neutron Source (SINQ), PSI, Switzerland. We acknowledge the outstanding technical support of W. Arrigoni, M. Meier and P. Schurter. We thank E. Widmann, A. Wokaun and J. Zmeskal for discussions. We acknowledge the support from Polish Ministry of Science and Higher Education, grant no. N N202 065436.

---

* Also at Inst. for Technical Chemistry, ETH Zürich, CH.
† Present address: Excellence Cluster Universe, Technical University Munich, Germany.
‡ Also at Physik-Institut, University of Zürich, CH
§ Also at Stefan Meyer Institut für subatomare Physik, Austrian Academy of Sciences, Vienna, Austria.; Present address: University of Fribourg, CH; Corresponding author, malgorzata.kasprzak@unifr.ch
¶ Corresponding author, klaus.kirch@psi.ch
** Also at Paul Scherrer Institut, CH-5232 Villigen PSI.

[1] A solid $^2H_2$ UCN source is in the commissioning phase at PSI, see A. Anghel *et al.*,Nucl. Instr. and Methods Phys. Res., Sect. A, **611**, 272 (2009). Other efforts are under way at Los Alamos National Lab, PNPI Gatchina, ILL Grenoble, RCNP Osaka, Mainz University, TU Munich, NC State University, TRIUMF and J-PARC.
[2] R. Golub, J. M. Pendlebury, Phys. Lett. **62A**, 337 (1977).
[3] R. Golub and K. Böning, Z. Phys. **B51**, 95 (1983).
[4] I. S. Altarev *et al.*, Phys. Lett. **80A**, 413 (1980).
[5] A. Serebrov *et al.*, Nucl. Instr. and Methods Phys. Res. **440**, 658 (2000).
[6] C. L. Morris *et al.*, Phys. Rev. Lett. **89**, 272501 (2002).
[7] A. Saunders *et al.*, Phys. Lett. **B 593**, 55 (2004).
[8] F. Atchison *et al.*, Phys. Rev. Lett. **94**, 212502 (2005).
[9] F. Atchison *et al.*, Phys. Rev. Lett. **95**, 182502 (2005).
[10] F. Atchison *et al.*, Phys. Rev. C **71**, 054601 (2005).
[11] F. Atchison *et al.*, Phys. Rev. Lett. **99** 262502 (2007).
[12] I. S. Altarev *et al.*, Phys. Rev. Lett. **100**, 014801 (2008).
[13] I. S. Altarev *et al.*, Eur. Phys. J. A **37**, 9 (2008).
[14] F. Atchison *et al.*, Nucl. Instr. and Methods Phys. Res., Sect. A, **611**, 252 (2009).
[15] V. K. Ignatovich, *The Physics of Ultracold Neutrons*, Clarendon Press, Oxford, 1990.
[16] C.-Y. Liu and A. R. Young, arXiv:nucl-th/0406004.
[17] Y. Pokotilovski, *ESS Special Expert Meeting*, http://www.ati.ac.at/~neutrweb/ess/8.pdf, Wien, 2002.
[18] C. A. Baker et al., Phys. Lett. A 308, 67 (2003).
[19] J. Zejma *et al.*, Nucl. Instr. and Methods Phys. Res., Sect. A **539**, 622 (2005).
[20] K. Bodek *et al.*, Nucl. Instr. and Methods Phys. Res., Sect. A **533**, 491 (2004).
[21] F. Atchison *et al.*, Nucl. Instr. and Methods Phys. Res. **552**, 513 (2005).
[22] C.-Y. Liu, A. R. Young, and S. K. Lamoreaux, Phys. Rev. B **62**, R3581 (2000).
[23] A. Frei *et al.*, arXiv:0911.4398v1 [nucl-ex].
[24] E. P. Shabalin *et al.*, Part. and Nuclei Letters No. 5 (114) (2002).